TENMAK BOREN

BOR DERGİSİ
JOURNAL OF BORON
https://dergipark.org.tr/boron

Zinc borate-mediated reduction of lipid droplets and cooperative suppression of clonogenic survival with mTOR inhibition in colorectal cancer cells

Selin Küçükparmaksız [1], **Işıl Özdemir** [1], **Aliye Ezgi Güleç Taşkıran** [1,*]

[1] *Başkent University, Faculty of Science and Letters, Molecular Biology and Genetics Department, Ankara, 06790, Türkiye*

ARTICLE INFO

Article History:
Received August 16, 2025
Accepted March 31, 2026
Available online June 30, 2026

Research Article

DOI: 10.30728/boron.1766217

Keywords:
Autophagy
Colorectal cancer
Lipid metabolism
Proliferation
Zinc borate

ABSTRACT

Colorectal cancer (CRC) is a leading cause of cancer-related deaths worldwide, with progression and metastasis closely tied to metabolic adaptations, including lipid storage and utilization. Boron derivatives have been shown to influence lipid metabolism in animals and humans. Oral boric acid, for example, reduces body weight in mice by inducing thermogenic proteins in adipose and skeletal muscle, promoting lipolysis. In this study, the anticancer potential of zinc borate (ZnB) in CRC cell lines SW480 (primary) and SW620 (metastatic) by modulating lipid storage investigated. ZnB reduced cell viability in a dose-dependent manner, with SW620 cells showing greater resistance. Fluorescence imaging indicated decreased lipid droplet (LD)-containing cells, consistent with possible lipophagy involvement. Colony formation and wound healing assays revealed impaired proliferation and migration, further diminished by the autophagy inducer AZD-8055. Under glutamine-deprived conditions-known to enhance lipid storage and aggressiveness-combined ZnB and AZD-8055 treatment markedly reduced LD content, proliferation and motility. These results suggest that ZnB disrupts lipid homeostasis involved in CRC cell survival. Our findings highlight the potential therapeutic value of co-targeting lipid metabolism and autophagy to combat metabolically adaptive and aggressive CRC.

1. Introduction

With the third common cancer worldwide and the second one of mortality, CRC has been an important public health issue in recent years [1]. By 2035, deaths from rectal and colon cancers are projected to rise by 60% and 71.5%, respectively [2].

Risk factors contributing to CRC include family history, genetic predispositions, inflammatory bowel disease, and the presence of colon polyps [3]. It is estimated that about 95% of CRC cases originate from abnormal epithelial lesions in the colorectal mucosa, known as adenomatous polyps [4].

CRC is a highly heterogeneous disease, with multiple molecular pathways driving tumor development and metastasis [5]. Cancer cells adapt their metabolism through a process called metabolic reprogramming, relying on aerobic glycolysis to produce energy even in oxygen-rich environments [6]. This phenomenon, known as the “Warburg Effect”, supports tumor growth under challenging conditions [7] and also impacts lipid metabolism [1], which is a key feature of CRC and other cancers [6]. Lipids serve as an alternative energy source and play a critical role in the metabolic flexibility of CRC [8]. As essential components for cell structure and energy storage, lipids are increasingly consumed by tumor cells under metabolic stress, often exceeding the rate at which they are synthesized [9]. By altering lipid metabolic pathways-including de novo lipogenesis (DNL), lipid transport, fatty acid oxidation, LD mobilization, and membrane remodeling-cancer cells enhance proliferation and migration while ensuring sufficient energy reserves for future demands [10,11].

Previous studies have shown that boron derivatives affect lipid metabolism in both rats and humans [12]. It has been demonstrated that orally administered boric acid accelerates lipolysis (the breakdown of lipids via autophagy) in mice through the overexpression of thermogenic proteins in adipose and skeletal muscle tissues, thereby reducing body weight [13]. After oral administration, borate is absorbed from the gastrointestinal tract and rapidly distributed to tissues, and it has been shown that boric acid administration in rats leads to increased mRNA expression of fatty acid transporters FATP1 and FATP44 in the jejunum [12]. The same study also demonstrated that boric acid administration reduces the levels of adipogenesis-related genes such as PPARγ, SREBP-1c, LxR-α, and FAS. Due to its effects on body weight and lipid metabolism, boric acid has even been suggested for use in diabetic patients [12].

*Corresponding author: aezgi1469@gmail.com

The Wnt/β-catenin signaling pathway is one of the most important pathways for adipogenic differentiation, and any suppression of its activity can cause an immediate negative effect in cells [14.] Boron treatment has been shown to stabilize β-catenin protein levels in precursor adipose cells, and this is proposed as the main underlying cause of boron's negative effects on adipogenesis [15]. In addition, by interacting with the NAD^+ molecule, boron has been reported to inhibit cyclic ADP-ribose, thereby reducing luminal endoplasmic reticulum Ca^{2+} levels and altering the endoplasmic reticulum calcium homeostasis, which is known to have an effect on adipogenic transformation [15].

Various forms of boron, which can form compounds with numerous molecules, have been used for therapeutic purposes on cancerous tissues [16]. There is a noticeable lack of research on the effects of boron-zinc compound derivatives, despite the known properties of zinc in reducing oxidative stress, increasing inflammatory cytokine levels, and suppressing tumor-promoting transcription factors [17]. Nevertheless, the effects of boron compounds on the lipid metabolism of cancer cells have not been thoroughly investigated. To our knowledge, this is the first study to investigate the effects of zinc borate (ZnB) on lipid metabolism and autophagy in CRC cells. Unlike other boron derivatives, ZnB offers the combined advantage of boron's metabolic regulation and zinc's antioxidant/anti-inflammatory properties, positioning it as a unique candidate for targeting metabolic vulnerabilities in CRC.

In this study, we examined the potential anticancer activity of ZnB against the CRC lines SW480 and SW620 by targeting lipid storage. To better understand whether the effects of ZnB on lipid metabolism and autophagy differ according to tumor stage, we utilized the isogenic CRC cell lines SW480 and SW620, both derived from the same patient. SW480 originates from the primary colon tumor, whereas SW620 was isolated from a lymph node metastasis. This pairing offers a unique model to directly compare primary versus metastatic CRC within the same genetic background. Previous studies, including our own, have demonstrated that SW620 cells display greater reliance on lipid metabolism under nutrient stress compared to SW480 [18]. By using these two lines, our objective was to investigate whether ZnB's modulation of lipid metabolism and autophagy could reveal stage-specific vulnerabilities, thereby providing insight into how metabolic targeting strategies may differentially affect primary and metastatic CRC. Our findings suggest that ZnB disrupts lipid homeostasis, a process essential for CRC cell survival, and that its therapeutic efficacy is augmented through autophagy activation highlighting the potential of co-targeting lipid metabolism and autophagy as an innovative strategy against metabolically adaptive, aggressive CRC.

2. Materials and Methods

2.1. Materials

Cells in L-Glutamine supplemented [(+) LG] or L-Glutamine deprived [(-) LG] medium were treated with pre-optimized concentrations of zinc borate (ZnB), 6-minonicotinamide (6-AN), AG-120, or AZD-8055 for 24h [18,19]. Information about the treatment duration and concentration is given in Table 1.

Table 1. Chemicals used in the study.

Chemical	Concentration	Duration	Vehicle	Company
ZnB	1μM-1mM	24h	DPBS	Eti Maden, 138265-88-0/12767-90-7
6-AN	100μM	24h	DMSO	Sigma Aldrich, A68203
AG-120	50μM	24h	DMSO	Cayman Chemical, 19894
AZD-8055	10μM	24h	DMSO	MedChem, 009298-09-2

For viability assays, ZnB was dissolved directly in the culture medium to avoid solvent-induced cytotoxicity at the high concentrations required for dose-response analyses. For all other assays, 1mM ZnB solution is prepared in sterile DPBS, and sterile DPBS in the same volume of ZnB applied was served as vehicle control. ZnB was a kind gift from Dr. Özge Erdemli, while 6-AN, AG-120, and AZD-8055 were kind gifts from Prof. Dr. Sreeparna Banerjee.

2.2. Cell Culture

SW480 and SW620 cells were kindly provided by Prof. Dr. Sreeparna Banerjee. Cells were maintained in Dulbecco's Modified Eagle Medium Low Glucose (DMEM, VivaCell, Germany) media supplemented with 10% fetal bovine serum (FBS, Capricorn Scientific, Germany), 2 mM L-glutamine (VivaCell, Germany), and 100 units/ml penicillin g sodium salt/100μg/ml streptomycin (VivaCell, Türkiye). For L-glutamine starvation, the cells were incubated for 24 h in L-glutamine-free medium.

2.3 Cell Viability Assay

3-(4,5-dimethylthiazol-2-yl)-2,5-diphenyltetrazolium bromide (MTT) and Resazurin Reduction assays were applied to determine cytotoxicity of ZnB and determine IC_{50} values. 10,000 cells in 100 μL were seeded in each well of 96-well plate. The day after, media was aspirated, and cells were treated with ZnB in the range of 1-1000 μM for 24h. For MTT assay upon completion of treatment, media containing ZnB were aspirated, and 100 μL media containing 1.2 mM MTT were added to each well. After 4 hours of incubation, 100 μL 10% SDS-0.01M HCl solution was added to each well, and plates were incubated for 16-18 hours at 37°C. The absorbance values were measured at 540nm using ELx800 Microplate Reader (BioTek Instruments, USA). Following blank subtraction, the absorbance

value of each treatment was normalized to the control (vehicle) group. For the Resazurin Reduction assay upon completion of treatment, 150 µg/mL resazurin were added to each well and left for 2.5h incubation at 37°C. The absorbance values were measured at 540 nm (resorufin) and 630 nm (background correction) using ELx800 Microplate Reader (BioTek Instruments, USA). The percentage of resazurin reduction was calculated by subtracting the 630 nm reading from 540 nm for each well, correcting for blank values, and normalizing to the untreated control.

2.4. Proliferation Assay

Colony formation assay was performed to evaluate the proliferation of the cells in response to the corresponding treatments. 1,000 cells in 1000 µL were seeded in each well of 6-well plate and left overnight for attachment. The following day, the media aspirated, and cells were treated with indicated treatments for 24h (Table 1). Sterile DPBS served as vehicle control. Upon completion of treatment, media in each well was aspirated, cells washed with sterile DPBS (VivaCell, Germany) and fresh media was added to each well. The culture medium was replaced every other day until colonies were visible to the naked eye (around 8 days). Cells were then washed once with DPBS (VivaCell, Germany) and fixed in 4% formaldehyde (ISOLAB, Germany) in PBS for 15 minutes at room temperature. Following fixation, the solution was removed, and the wells were washed once more with PBS. Subsequently, 1 ml of 0.5% crystal violet solution (Amresco, USA), prepared in 80% distilled water and 20% methanol, was added and incubated for 20 minutes at room temperature on a bench rocker. Plates were then gently rinse four times with tap water and left to air-dry overnight uncovered. The next day, the staine colonies were imaged using the G:Box Chemi XRQ system (Syngene, India).

2.5. Lipid Droplet Staining

300,000 cells per well were seeded on a 6-well plate and left overnight for attachment. The following day indicated treatments were applied in (+) or (-) LG medium. Upon completion of treatment (24h), cells were fixed with 4% formaldehyde in PBS for 20 min, and nile red (GlpBio Technology Inc., USA) staining was applied for 30 min to label neutral lipid accumulating in LDs. Following washing steps, cells were imaged using DMi8 Inverted Microscope (Leica Microsystems, Germany) equipped with HC PL FLUOTAR 10x/0.30 objective and L5/GFP filter cube (Ex: 488 nm/Em: 525 nm). Images were processed in Fiji (https://fiji.sc), and cells containing and not containing LDs were counted manually, and the percentage of LD-containing cells was calculated based on this counting.

2.6. Scratch Assay

The wound healing (scratch) assay was performed to determine the effect of a compound on cell migration. 1,500,000 cells per well were seeded on a 6-well plate and left overnight for attachment. The following day, wounds were generated using a sterile micropipette tip in the cell culture media. To suppress the cell proliferation, cells were treated with 0.5 µM mitomycin C. Later on, cells were washed with 1X DPBS (VivaCell, Germany), and indicated treatments were applied in (+) or (-) LG medium. Wounds were imaged using DMi8 Inverted Microscope equipped with HC PL FLUOTAR 10x/0.30 objective in white light setting at 0h, 24h, and 48h. The length of a scratch was measured by using Fiji.

2.7. Statistical Analysis

Statistical analyses were carried out using GraphPad Prism Version 8.0 (GraphPad Software, USA). A linear regression curve was used for the determination of IC_{50} using MTT assay results. IC_{50} values of two cell lines were compared by t-test. 2-Way ANOVA was applied to analyze the colony formation, LD staining, and wound healing assays to compare both the effects of treatments and cell line differences. $P<0.05$ was taken as an indication of statistical significance.

3. Results and Discussion

SW480 and SW620 cell lines were treated with increasing concentrations of ZnB for 24h, and the viability of the cells was determined using the MTT assay. ZnB treatment exhibited a dose-dependent decrease in the viability of both cell lines, SW620 cell line being slightly more resistant to ZnB treatment. IC_{50} values were determined in the 1-1000 µM range using 15 different doses and were calculated as 212.8 µM for SW480 and 303.3 µM for SW620 cells (Figure 1a). As can be seen in Figure 1b, the IC_{50} values of the cell lines, which were calculated from different biological replicates, are analyzed with t-test and indicated a trend toward higher IC_{50} in SW620 compared with SW480 ($p=0.067$). Additionally, resazurin viability test was applied using different doses of ZnB at 24- and 48-h treatment duration to compare differential responses to cell lines to ZnB treatment. SW480 cells exhibit a decrease in resazurin reduction in response to increasing ZnB concentration, while SW620 cells exhibit persistence in reduction in both time points (Figure 1c). Best to our knowledge, there is not any available data comparing the cytotoxic effects of ZnB on SW480 and SW620 cell lines. Yet, various studies indicate that SW620 are less sensitive to chemotherapy agents compared to SW480 cells [20-22]. SW620 cells found to have higher IC_{50} values for oxaliplatin, irinotecan and 5-flurouracil which are commonly employed therapy options for the treatment of CRC [21-23]. Additionally, several studies demonstrated the use of boric acid and zinc derivates against colorectal cancer cell lines. For example, boric acid was shown to possess antiproliferative and apoptotic effects against SW480 cells, the testes concentration range includes 10-100mM [24]. In another study, IC_{50} value of boric acid derivate sodium tetraborate was determined as

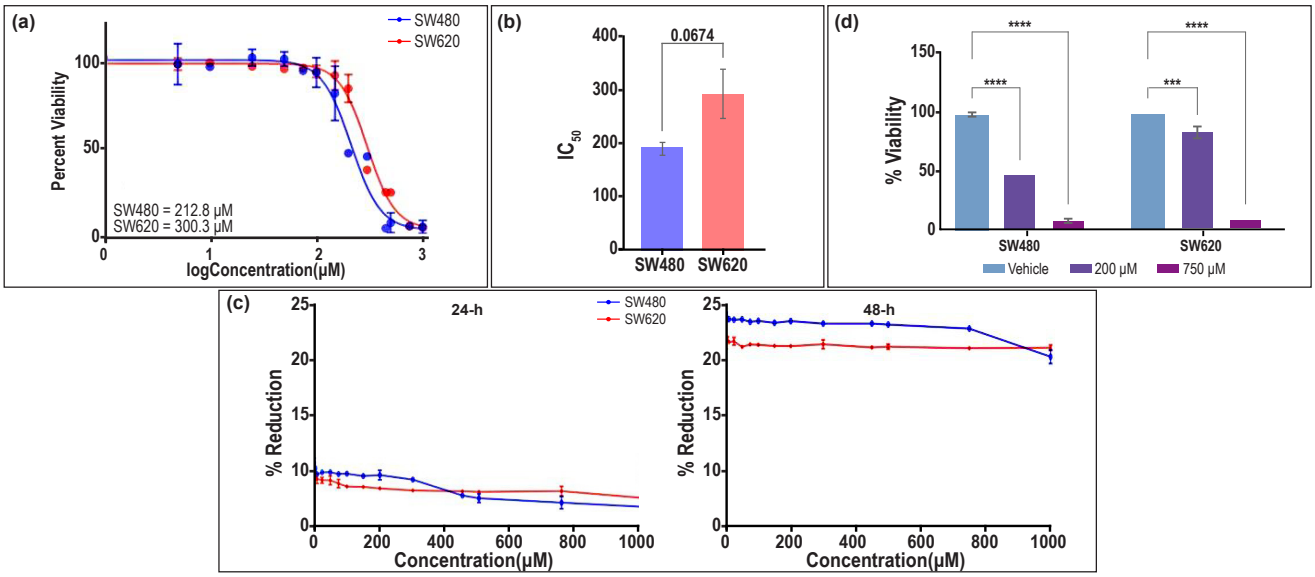

Figure 1. ZnB treatment leads to a dose-dependent response in SW480 and SW620 cells. (A) Determination of IC_{50} values of ZnB in SW480 and SW620 cell lines using MTT viability assay. (B) Comparison of IC_{50} values calculated in different biological replicates in both cell lines. (C) Resazurin viability test indicating the differential responses of cell lines to ZnB treatment in 24- and48- treatment durations. (D) ZnB Determination of viable cell percentage in response to 200 µM and 750 µM ZnB treatment. Three biological replicates were used, and the data are represented as the mean ± SEM. IC_{50} values in panel B were compared by t-test; resazurin data in panel C and D were analyzed by two-way ANOVA with factors X [cell line] and Y [dose]. The error bars representing SEM are very small in some conditions, leading to difficulty in visual observation. ***p<0.001, ****p < 0.0001, two-way ANOVA.

500 µM at 24h [25]. Uçar et al. demonstrated that zinc (II) complex exhibits anticancer effects against HT-29 CRC cells with an IC_{50} of 17.03 µg/ml [26]. Collectively, the MTT-based IC_{50} values obtained in this study are in agreement with previously published reports demonstrating cytotoxic effects of boric acid and zinc derivatives in colorectal cancer cell lines, as well as with studies reporting reduced chemosensitivity of the metastatic SW620 cell line compared to the primary tumor- derived SW480 cells.

Two doses were selected for further analysis as 200 µM, which is near the IC_{50} for SW480 but below the IC_{50} for SW620, and 750 µM, which exhibits low viability in both cell lines (Figure 1d). These doses were chosen empirically from the dose-response curves as moderate and high concentrations rather than as IC_{50} doses for both cell lines. Using the same dose allowed us to assess how primary versus metastatic cells respond to equivalent pharmacological pressure, rather than normalizing responses solely based on cytotoxicity. The higher concentration (750 µM) was intentionally selected as a supra-IC_{50} dose for both cell lines to probe the upper limit of the compound's biological activity.

To determine the effect of ZnB treatment on lipid droplet abundance, Nile Red staining was applied using two selected doses. Nile Red stains the neutral lipids and accumulated neutral lipids in LDs exhibit a puncta formation. Both doses of ZnB lead to a decrease in LD-containing cell percentages in both cell lines, consistent with a possible involvement of lipophagic activity, decreased lipid synthesis or enhanced lipid oxidation (Figure 2). Since 750 µM ZnB-treated cells exhibited a dramatic morphological change, and decreased viability, this dose is eliminated in further studies to eliminate the pronounced effect led by cell death. To our knowledge, there exists no available data on the effects of ZnB treatment on the LD abundance of CRC cells. Yet, there are many studies highlights the deregulated lipid metabolism (elevated fatty acid uptake, elevated fatty acid synthesis), enhanced LD abundance in cancer cells promoting the cancer progression. For example, high expression of fatty acid translocase (CD36) has been linked to the higher proliferative and migratory capacity of HT-29 and HCT-116 CRC cell lines [27,28]. Elevated lipid storage in LD has been linked to the EMT and metastatic spreading of cancer cells [29]. Even though there is no direct evidence linking the zinc or boric acid derivates to lipid storage in LD, oral boric acid intake was linked to increased thermogenesis, and subsequent lipolysis [13]. Therefore, the observed decrease in LD-abundance in response to ZnB treatment correlates with the literature.

Our earlier findings demonstrated that L-glutamine deprivation led to elevated LD levels in both cell lines, with cellular uptake identified as the primary lipid source [18]. Increased LD content was accompanied by sustained proliferation and enhanced cell motility, particularly in the metastatic SW620 cell line [18]. Furthermore, previous studies have consistently reported that serum glutamine concentrations are reduced in CRC patients compared with healthy controls [30,31]. Based on these findings, a colony formation assay was conducted using ZnB treated cells under both glutamine-rich and glutamine-deprived conditions to investigate whether ZnB treatment could suppress long-term clonogenic growth (long-term proliferation capacity) under glutamine-rich and

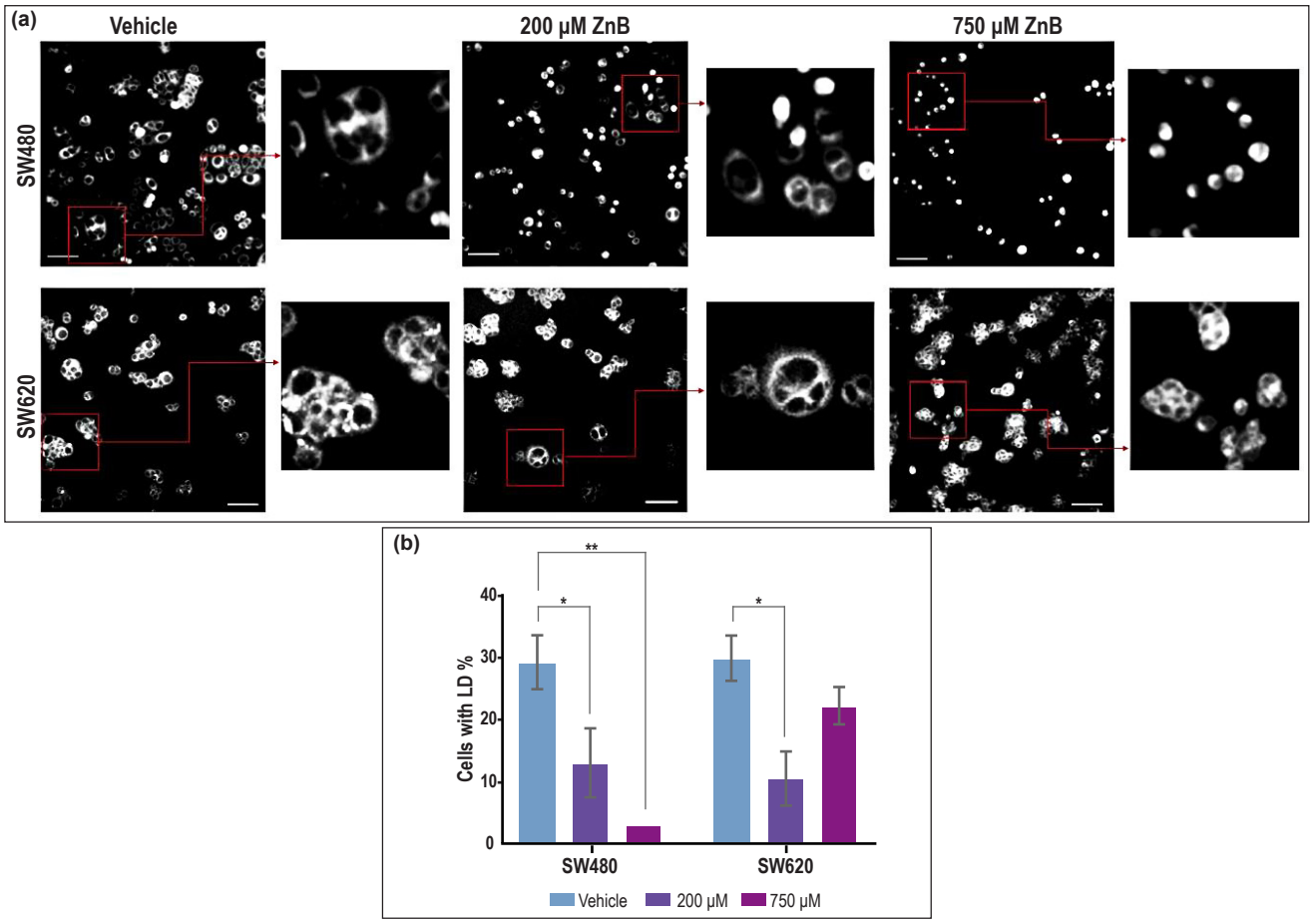

Figure 2. ZnB treatment leads to a decrease in the LD-containing cell percentages of SW480 and SW620 cells. (A) Representative microscopy images of Nile Red staining. The bar correspond to 100 µm. 3X zoomed-in images are provided on the right-hand side, the rectangle indicates the region zoomed in. (B) Bar graph represents the percentage of LD-containing cells to total cell number. Two biological replicates were used, and the data are described as the mean ± SEM. *p < 0.05, **p < 0.01, two-way ANOVA. Raw images are provided in Supplementary Figure 1.

glutamine-deprived conditions. To further elucidate the relationship between ZnB treatment and metabolic or autophagic regulation, cells were exposed to ZnB in combination with NADPH production inhibitors-6-AN (a pentose phosphate pathway inhibitor) and AG-120 (an isocitrate dehydrogenase inhibitor)-as well as with the mTOR inhibitor AZD-8055, which induces autophagy. The individual effects of 6-AN, AG-120, and AZD-8055 on colony formation were also examined to allow for direct comparison with the combination treatments.

While LD levels were not directly quantified under these experimental conditions, the observed alterations in colony formation capacity may suggest a potential association with changes in lipid metabolism. ZnB alone significantly reduced colony formation in SW480 cells specifically under L-glutamine-deprived conditions, whereas SW620 cells showed only a moderate decrease (Figure 3a-b). Notably, co-treatment with AZD-8055 and ZnB led to a pronounced suppression of colony formation, most prominently under L-glutamine-deprived conditions in both cell lines (Figure 3a-b). While AZD-8055-induced autophagy was observed, confirmation of whether this process specifically represents lipophagy requires further investigation using additional autophagy- and lipophagy-related markers. In addition, combined treatment with AG-120 or 6-AN together with ZnB selectively suppressed the colony-forming capacity of SW480 cells under L-glutamine-deprived conditions, whereas ZnB alone produced more limited and condition-dependent effects. These findings suggest a possible role for lipid biosynthesis in supporting clonogenic survival in SW480 cells. Importance of fatty acid synthesis for CRC proliferation and metastasis has been implicated in many recent studies which are in line with our findings [32,33].

To further understand the involvement of LD abundance in response to ZnB and AZD-8055 treatment, Nile Red staining was performed on ZnB- and AZD-8055-treated cells. ZnB treatment significantly decreased LD-containing cells in glutamine-rich conditions for both lines and in glutamine-deprived SW620 cells (ns in SW480 glutamine-deprived). The reduction in LD-containing cell percentage of SW480 was found to be 15.9% (p=0.0297) in glutamine-containing media (Figure 4b upper panel left-hand side) and 5.3% (ns) in glutamine deprived media (Figure 4b upper panel right-hand side). The reduction in LD-containing cell percentage of SW620 was found to be 17.3% (p=0.0210) in glutamine-containing media (Figure 4b

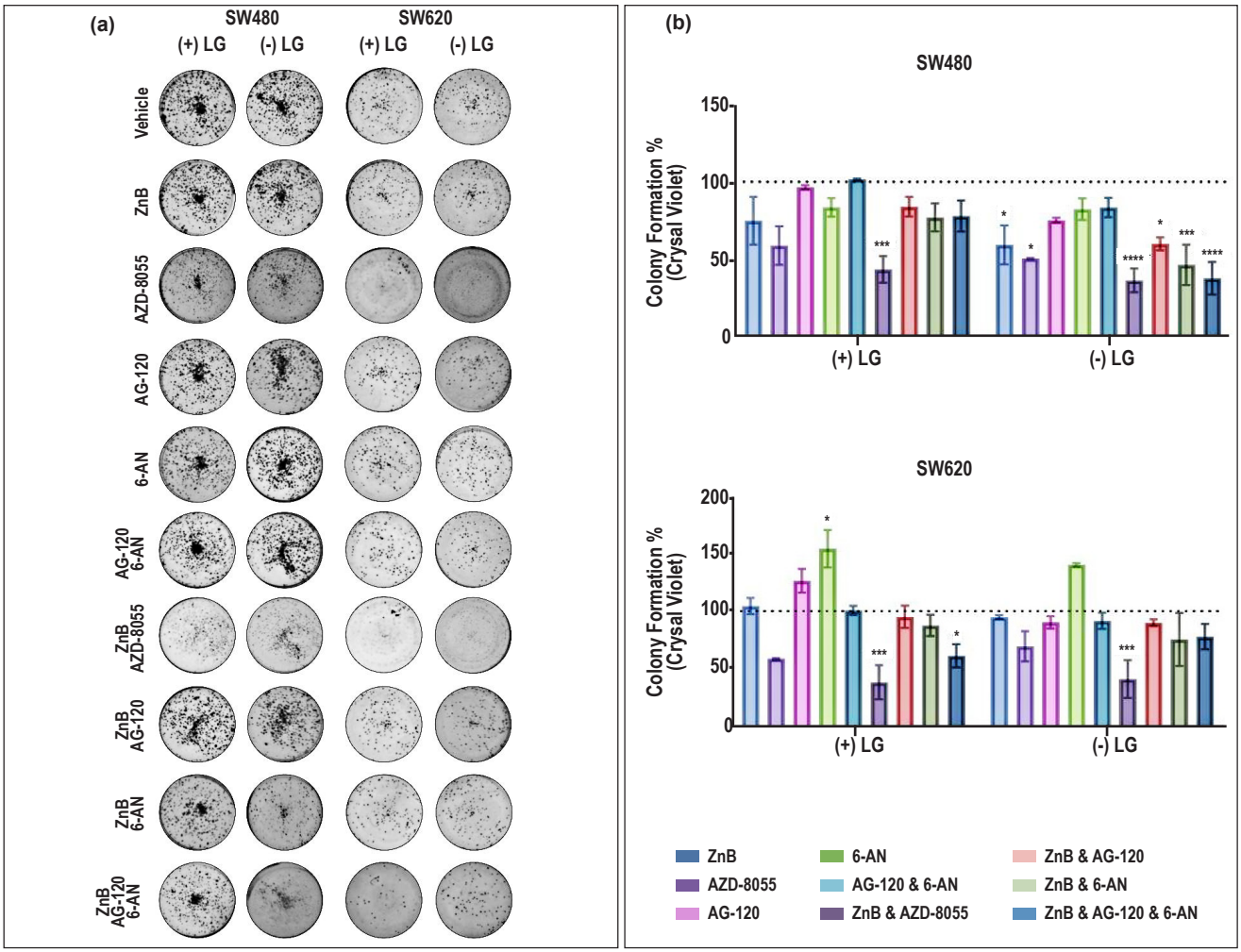

Figure 3. ZnB treatment, combined with the autophagy inducer AZD-8055, results in a pronounced reduction in colony formation in SW480 and SW620 cells. (A) Representative colony images of crystal violet staining of colonies. (B) Bar graph representing the percentage of colony formation capacity. The data was normalized to the vehicle control, which is indicated by the dashed line. Three biological replicates were used, and the data are described as the mean ± SEM. *p < 0.05, **p < 0.01, ****p < 0.0001, two-way ANOVA.

lower panel left-hand side) and 10.9% (p=0.0282) in glutamine deprived media (Figure 4b lower panel right-hand side). The decrease in LD-containing cells as opposed to the vehicle treated cells was more dramatic when the combinatorial treatment applied especially for the case of SW620 cells in glutamine deprived media. 6.2% decrease in LD-containing cells was observed in glutamine-deprived SW620 cells when AZD-8055 combinatorial treatment applied compared to ZnB treatment alone (Figure 4b lower panel right-hand side). Considering that autophagy induction has been previously linked to the clearance of LD from cells, the more pronounced effects observed in combination with an autophagy inducer correlate with a potential involvement of lipophagy, although further mechanistic studies are required [34,35].

Enhanced lipid storage within the cancer cells has been linked to cell survival and metastasis [36]. Taken together with the LD data, these findings suggest that modulation of cell survival by ZnB and AZD-8055 may involve reduced lipid storage. To underscore the role of lipid storage in migratory behavior, a wound healing assay was conducted in ZnB- and AZD-8055-treated cells. Figure 5 exhibits representative images illustrate the progressive closure of the scratch area over 0, 24, and 48 hours, while the accompanying quantitative analyses present both time-course and endpoint measurements of wound closure. In SW480 cells, treatment tended to reduce migration compared with vehicles under both nutrient conditions, although the differences were not statistically significant. In SW620 cells, the inhibitory effect of treatment on wound closure was more pronounced. Both ZnB as single agent (p=0.0257) and in combination with AZD-8055 (p=0.0050) was able to decrease the wound closure significantly compared to Vehicle at 48h time point. ZnB and AZD-8055 combinatorial treatment were also able to suppress migration of SW620 cells in glutamine-rich media at 24h time point (p=0.0294). Considering that glutamine starvation enhances LD formation, results suggest that SW620 cells may rely on lipid storage to support motility under glutamine deprivation. Importance of lipid storage for migratory behavior has been shown by various studies as well. A systematic review analyzing the 12,837 CRC patient data underscores the importance of abdominal obesity for the progression of CRC [37]. In another

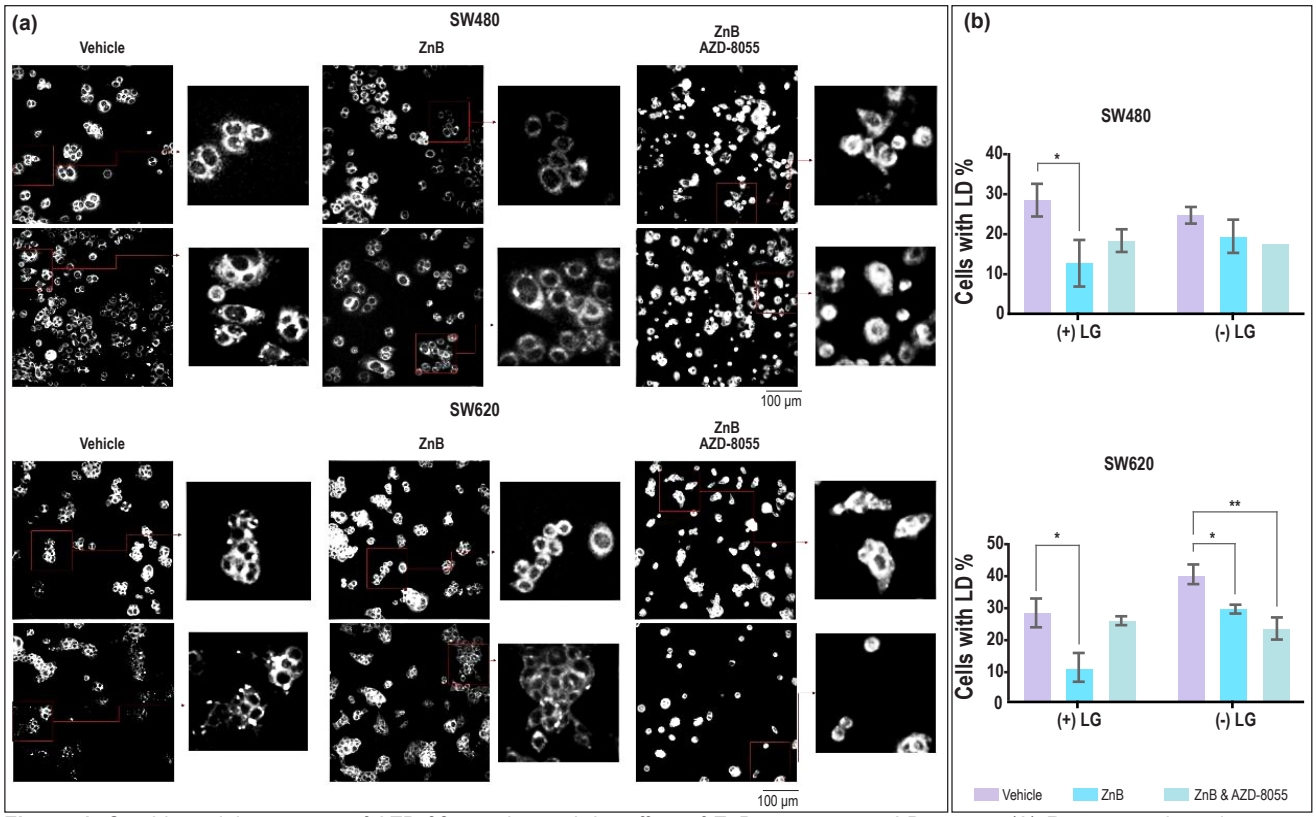

Figure 4. Combinatorial treatment of AZD-0855 enhanced the effect of ZnB treatment on LDcontent. (A) Representative microscopy images of Nile Red staining. 3X zoomed-in images. The bar corresponds to 100 µm. 3X zoomed-in images are provided on the right-hand side, the rectangle indicates the region zoomed in. (B) Bar graph represents the percentage of LD-containing cells to total cell number. Two biological replicates were used, and the data are described as the mean ± SEM. *p < 0.05, **p < 0.01, ****p < 0.0001, two-way ANOVA. Raw images are provided in Supplementary Figure 1.

study, LD has been shown as a key resource to fuel the metastasis process through the oncogene KRAS in human pancreatic cancer cells [38]. Additionally, AZD-8055 is a well-known autophagy inducer through mTOR inhibitor, and its role has been exemplified by many studies [39,40]. Xie et al. demonstrated the role of mTORC1 for the suppression of lipophagy in a RAB7-A dependent manner as well linked the suppression of mTOR with decreased lipid storage and therefore limitation of the migratory behavior [41].

Collectively, ZnB disrupts lipid storage and, in combination with AZD-8055, reduces colony formation, LD content, and motility (primarily in SW620 cells under glutamine deprivation), suggesting a potential role for lipid metabolism in CRC cell survival (Figure 6). These findings highlight the therapeutic potential of targeting lipid metabolism to impair cancer cell survival and aggressiveness.

4. Conclusions

In this study, the impact of ZnB treatment on CRC lines SW480 and SW620, with a focus on cell viability, lipid metabolism, and proliferative and migratory behavior investigated. ZnB treatment reduced cell viability in a dose-dependent manner, with SW620 cells displaying greater resistance than SW480 cells. Selected doses of ZnB significantly decreased the percentage of LD-containing cells, suggesting potential lipophagic activity, decreased lipid synthesis or enhanced lipid oxidation. Although these changes may indicate a link with lipid metabolism and ZnB treatment, further studies are required to confirm the effect on ZnB treatment on lipid biosynthesis, lipophagic activity or lipid peroxidation. Colony formation and wound healing assays demonstrated ZnB reduces LD content primarily in glutamine-rich conditions and impairs motility in glutamine-deprived SW620 cells, effect enhanced by AZD-8055 combination, suggesting a potential role for lipid mechanism in CRC adaptation under glutamine stress. However, the absence of additional dedicated motility and invasion assays (such as transwell-based approaches) represents a limitation of the present study and should be addressed in future work. Notably, the combined treatment significantly reduced LD content, particularly under glutamine-deprived conditions, which previously were shown to elevate LD accumulation and support cancer cell proliferation and motility [18].

These findings suggest that ZnB alters lipid storage and/or utilization, which may contribute to CRC cell adaptation. The enhanced effects observed when ZnB is combined with AZD-8055 are consistent with a possible role of lipid metabolism and storage pathways in supporting survival, particularly in metastatic-like cells that may rely more heavily on lipid reservoirs under metabolic stress.

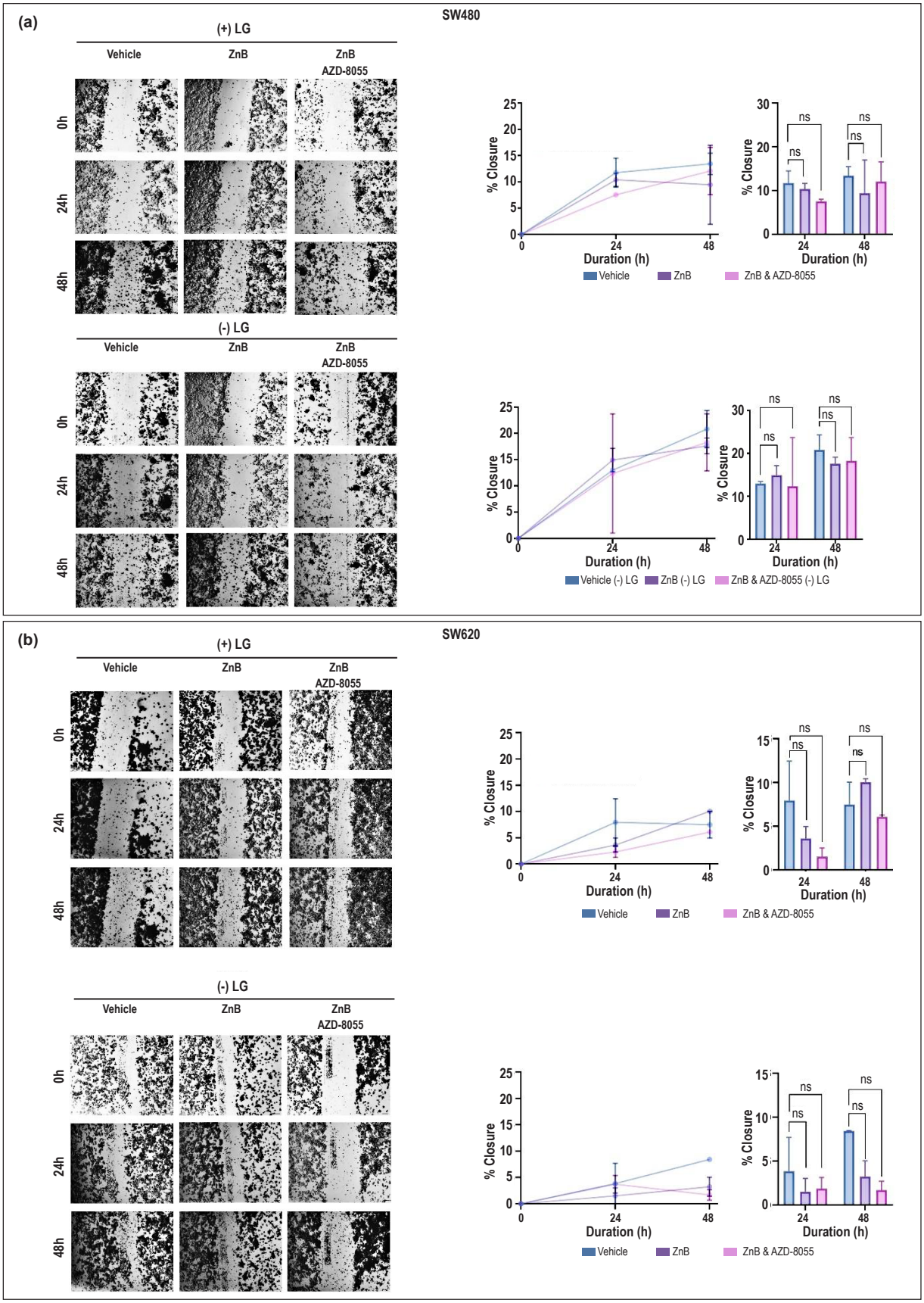

Figure 5. Combinatorial treatment of AZD-0855 enhanced the effect of ZnB treatment on motility. (A) Representative microscopy images of wounds (left panel), XY-graph indicatingthe time-course wound closure percentage (middle panel), and endpoint bar graph (right panel) are given for SW480 cells. (B) Representative microscopy images of wounds (left panel), XY-graph indicating the time-course wound closure percentage (middle panel), and endpoint bar graph (right panel) are given for SW620 cells. Two biological replicates were used, and the data are described as the mean ± SEM. *$p < 0.05$, **$p < 0.01$, two-way ANOVA. Representative raw images are provided in Supplementary Figure 2.

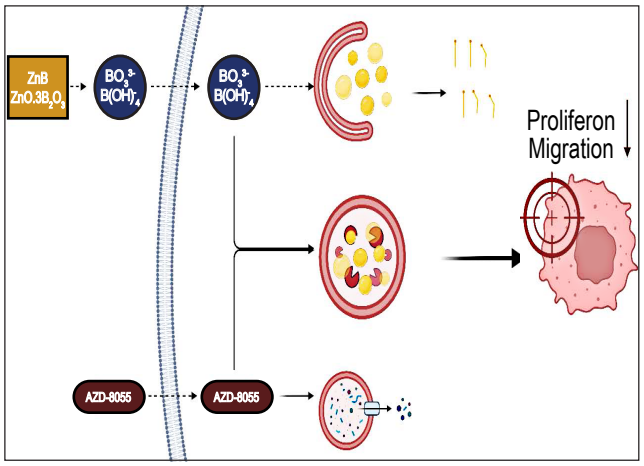

Figure 6. ZnB treatment disrupts lipid storage and reduces viability, proliferation, and motility in CRC cells, with enhanced effects observed when combined with autophagy induction via AZD-8055.

5. Acknowledgement

The study was funded by TÜBİTAK 2209-A (1919B012419083) to Selin Küçükparmaksız and Aliye Ezgi Güleç Taşkıran.

6. Author Contribution Statement

Selin Küçükparmaksız: Investigation, formal analysis, data curation, funding, writing original draft.

Işıl Özdemir: Investigation, formal analysis, data curation, writing original draft.

Aliye Ezgi Güleç Taşkıran: Investigation, formal analysis, data curation, writing original draft, supervision, resources, conceptualization.

7. Conflict of Interest

Authors have no conflict of interest.

References

[1] Salita, T., Rustam, Y. H., Mouradov, D., Sieber, O. M., & Reid, G. E. (2022). Reprogrammed lipid metabolism and the lipid-associated hallmarks of colorectal cancer. *Cancer*, *14*(15), 3714. https://doi.org/ 10.3390/cancers14153714

[2] Sawicki, T., Ruszkowska, M., Danielewicz, A., Niedźwiedzka, E., Arłukowicz, T., & Przybyłowicz, K. E. (2021). A review of colorectal cancer in terms of epidemiology, risk factors, development, symptoms and diagnosis. *Cancers*, *13*(9), 2025. https://doi.org/10.3390/cancers13092025

[3] Roshandel, G., Ghasemi-Kebria, F., & Malekzadeh, R. (2024). Colorectal cancer: Epidemiology, risk factors, and prevention. *Cancer*, *16*(8), 1530. https://doi.org/10.3390/cancers16081530

[4] Thelin, C. (2015). Epidemiology of colorectal cancer-incidence, lifetime risk factors statistics and temporal trends. In R. Ettarh (Ed.), *Screening for colorectal cancer with colonoscopy*. IntechOpen. https://doi.org/10.5772/61945

[5] Abedizadeh, R., Majidi, F., Khorasani, H. R., Abedi, H., & Sabour, D. (2024). Colorectal cancer: A comprehensive review of carcinogenesis, diagnosis, and novel strategies for classified treatments. *Cancer and Metastasis Reviews*, *43*(2), 729-753. https://doi.org/10.1007/s10555-023-10158-3

[6] Pakiet, A., Kobiela, J., Stepnowski, P., Sledzinski, T., & Mika, A. (2019). Changes in lipids composition and metabolism in colorectal cancer: A review. *Lipids in Health and Disease*, *18*(1), 29. https://doi.org/10.1186/s12944-019-0977-8

[7] Zhong, X., He, X., Wang, Y., Hu, Z., Huang, H., Zhao, S., … & Li, D. (2022). Warburg effect in colorectal cancer: The emerging roles in tumor microenvironment and therapeutic implications. *Journal of Hematology & Oncology*, *15*(1), 160. https://doi.org/10.1186/s13045-022-01358-5

[8] Nenkov, M., Ma, Y., Gaßler, N., & Chen, Y. (2021). Metabolic reprogramming of colorectal cancer cells and the microenvironment: Implication for therapy. *International Journal of Molecular Sciences*, *22*(12), 6262. https://doi.org/10.3390/ijms22126262

[9] Martin-Perez, M., Urdiroz-Urricelqui, U., Bigas, C., & Benitah, S. A. (2022). The role of lipids in cancer progression and metastasis. *Cell Metabolism*, *34*(11), 1675-1699. https://doi.org/10.1016/j.cmet.2022.09.023

[10] Vasseur, S., & Guillaumond, F. (2022). Lipids in cancer: A global view of the contribution of lipid pathways to metastatic formation and treatment resistance. *Oncogenesis*, *11*(1), 46. https://doi.org/10.1038/s41389-022-00420-8

[11] Vishwa, R., BharathwajChetty, B., Girisa, S., Aswani, B. S., Alqahtani, M. S., Abbas, M., … & Kunnumakkara, A. B. (2024). Lipid metabolism and its implications in tumor cell plasticity and drug resistance: What we learned thus far? *Cancer Metastasis Reviews*, *43*(1), 293-319. https://doi.org/10.1007/s10555-024-10170-1

[12] Şahin, E., Orhan, C., Erten, F., Şahin, F., Şahin, N., & Şahin, K. (2023). The effect of different boron compounds on nutrient digestibility, intestinal nutrient transporters, and liver lipid metabolism. *Turkish Journal of Medical Sciences*, 53(3), 619-629. https://doi.org/10.55730/1300-0144.5624

[13] Aysan, E., Sahin, F., Telci, D., Erdem, M., Muslumanoglu, M., Yardımcı, E., & Bektasoglu, H. (2013). Mechanism of body weight reducing effect of oral boric acid intake. *International Journal of Endocrinology*, *2013*, 914651. https://doi.org/10.1155/2013/914651

[14] Prestwich, T. C., & Macdougald, O. A. (2007). Wnt/beta-catenin signaling in adipogenesis and metabolism. *Current Opinion in Cell Biology*, *19*(6), 612-617. https://doi.org/10.1016/j.ceb.2007.09.014

[15] Doğan, A., Demirci, S., Apdik, H., Bayrak, O. F., Gulluoglu, S., Tuysuz, E. C., … & Şahin, F. (2017). A new hope for obesity management: Boron inhibits adipogenesis in progenitor cells through the Wnt/β-catenin pathway. *Metabolism: Clinical and Experimental*, *69*, 130-142. https://doi.org/10.1016/j.metabol.2017.01.021

[16] Kulkarni, S., Bhandary, D., Singh, Y., Monga, V., & Thareja, S. (2023). Boron in cancer therapeutics: An overview. *Pharmacology & Therapeutics*, *251*, 108548. https://doi.org/10.1016/j.pharmthera.2023.108548

[17] Prasad, A. S., & Bao, B. (2019). Molecular mechanisms of zinc as a pro-antioxidant mediator: Clinical therapeutic implications. *Antioxidants* (*Basel, Switzerland*), *8*(6), 164. https://doi.org/10.3390/antiox8060164

[18] Güleç Taşkıran, A. E., Karaoğlu, D. A., Eylem, C. C., Ermiş, Ç., Güderer, İ., Nemutlu, E., … & Banerjee, S. (2024). Glutamine withdrawal leads to the preferential activation of lipid metabolism in metastatic colorectal cancer. *Translational Oncology*, *48*, 102078. https://doi.org/10.1016/j.tranon.2024.102078

[19] Oral, G. (2023). *Activation of survival pathways in nutrient restricted colorectal cancer cells* (Publication No. 779228) [Master's thesis, Middle East Technical University]. https://hdl.handle.net/11511/101975

[20] Slater, C., De La Mare, J. A., & Edkins, A. L. (2018). In vitro analysis of putative cancer stem cell populations and chemosensitivity in the SW480 and SW620 colon cancer metastasis model. *Oncology Letters*, *15*(6), 8516-8526. https://doi.org/10.3892/ol.2018.8431

[21] Skarkova, V., Kralova, V., Krbal, L., Matouskova, P., Soukup, J., & Rudolf, E. (2018). Oxaliplatin and irinotecan induce heterogenous changes in the EMT markers of metastasizing colorectal carcinoma cells. *Experimental Cell Research*, *369*(2), 295-303. https://doi.org/10.1016/j.yexcr.2018.05.032

[22] Gao, L., Shen, L., Yu, M., Ni, J., Dong, X., Zhou, Y., & Wu, S. (2014). Colon cancer cells treated with 5 fluorouracil exhibit changes in polylactosamine type N glycans. *Molecular Medicine Reports*, *9*(5), 1697-1702. https://doi.org/10.3892/mmr.2014.2008

[23] Kawai, S., Takeshima, N., Hayasaka, Y., Notsu, A., Yamazaki, M., Kawabata, T., … & Yasui, H. (2021). Comparison of irinotecan and oxaliplatin as the first-line therapies for metastatic colorectal cancer: A meta-analysis. *BMC Cancer*, *21*(1), 116. https://doi.org/10.1186/s12885-021-07823-7

[24] Sevimli, M., Bayram, D., Özgöçmen, M., Armağan, I., & Semerci Sevimli, T. (2022). Boric acid suppresses cell proliferation by TNF signaling pathway mediated apoptosis in SW-480 human colon cancer line. *Journal of Trace Elements in Medicine and Biology : Organ of the Society for Minerals and Trace Elements (GMS)*, *71*, 126958. https://doi.org/10.1016/j.jtemb.2022.126958

[25] Kırlangıç, Ö. F., Kaya-Sezginer, E., Ören, S., Gür, S., Yavuz, Ö., & Özgürtaş, T. (2022). Cytotoxic and apoptotic effects of the combination of borax (sodium tetraborate) and 5-fluorouracil on DLD-1 human colorectal adenocarcinoma cell line. *Turkish Journal of Pharmaceutical Sciences*, *19*(4), 371-376. https://doi.org/10.4274/tjps.galenos.2021.29726

[26] Uçar, A., Çelik, S., & Pehlivanoğlu, S. (2024). Investigation of the anticancer activity of zinc(II) complex containing Schiff base on colorectal cancer cell. *Gümüşhane Üniversitesi Fen Bilimleri Dergisi*, *14*(4), 1039-1048. https://doi.org/10.17714/gumusfenbil.1486484

[27] Drury, J., Rychahou, P. G., He, D., Jafari, N., Wang, C., Lee, E. Y., … & Zaytseva, Y. Y. (2020). Inhibition of fatty acid synthase upregulates expression of CD36 to sustain proliferation of colorectal cancer cells. *Frontiers in Oncology*, *10*, 1185. https://doi.org/10.3389/fonc.2020.01185

[28] Drury, J., Rychahou, P. G., Kelson, C. O., Geisen, M. E., Wu, Y., He, D., … & Zaytseva, Y. Y. (2022). Upregulation of CD36, a fatty acid translocase, promotes colorectal cancer metastasis by increasing MMP28 and decreasing E-cadherin expression. *Cancers*, *14*(1), 252. https://doi.org/10.3390/cancers14010252

[29] Corbet, C., Bastien, E., Santiago de Jesus, J. P., Dierge, E., Martherus, R., Vander Linden, C., … & Feron, O. (2020). TGFβ2-induced formation of lipid droplets supports acidosis-driven EMT and the metastatic spreading of cancer cells. *Nature Communications*, *11*(1), 454. https://doi.org/10.1038/s41467-019-14262-3

[30] Zhu, J., Djukovic, D., Deng, L., Gu, H., Himmati, F., Chiorean, E. G., & Raftery, D. (2014). Colorectal cancer detection using targeted serum metabolic profiling. *Journal of Proteome Research*, *13*(9), 4120-4130. https://doi.org/10.1021/pr500494u

[31] Tan, B., Qiu, Y., Zou, X., Chen, T., Xie, G., Cheng, Y., … & Jia, W. (2013). Metabonomics identifies serum metabolite markers of colorectal cancer. *Journal of Proteome Research*, *12*(6), 3000-3009. https://doi.org/10.1021/pr400337b

[32] Lu, T., Sun, L., Wang, Z., Zhang, Y., He, Z., & Xu, C. (2019). Fatty acid synthase enhances colorectal cancer cell proliferation and metastasis via regulating AMPK/mTOR pathway. *OncoTargets and Therapy*, *12*, 3339-3347. https://doi.org/10.2147/OTT.S199369

[33] Wang, H., Xi, Q., & Wu, G. (2016). Fatty acid synthase regulates invasion and metastasis of colorectal cancer via Wnt signaling pathway. *Cancer Medicine*, *5*(7), 1599-1606. https://doi.org/10.1002/cam4.711

[34] Kaini, R. R., Sillerud, L. O., Zhaorigetu, S., & Hu, C. A. (2012). Autophagy regulates lipolysis and cell survival through lipid droplet degradation in androgen-sensitive prostate cancer cells. *The Prostate*, *72*(13), 1412-1422. https://doi.org/10.1002/pros.22489

[35] Xu, G., Jiang, Y., Xiao, Y., Liu, X. D., Yue, F., Li, W., … & Liu, L. (2016). Fast clearance of lipid droplets through MAP1S-activated autophagy suppresses clear cell renal cell carcinomas and promotes patient survival. *Oncotarget*, *7*(5), 6255-6265. https://doi.org/10.18632/oncotarget.6669

[36] Martin-Perez, M., Urdiroz-Urricelqui, U., Bigas, C., & Benitah, S. A. (2021). Lipid metabolism in metastasis and therapy. *Current Opinion in. System Biology*, *28*, 100401. https://doi.org/10.1016/j.coisb.2021.100401

[37] Dong, Y., Zhou, J., Zhu, Y., Luo, L., He, T., Hu, H., … & Teng, Z. (2017). Abdominal obesity and colorectal cancer risk: Systematic review and meta-analysis of prospective studies. *Bioscience Reports*, *37*(6), BSR20170945. https://doi.org/10.1042/BSR20170945

[38] Rozeveld, C. N., Johnson, K. M., Zhang, L., & Razidlo, G. L. (2020). KRAS controls pancreatic cancer cell lipid metabolism and invasive potential through the lipase HSL. *Cancer Research*, *80*(22), 4932-4945. https://doi.org/10.1158/0008-5472.CAN-20-1255

[39] Sánchez-Vidaña, D. I., Li, J., Abokyi, S., Chan, J. N., Ngai, S. P., & Lau, B. W. (2023). In vitro methods in autophagy research: Applications in neurodegenerative diseases and mood disorders. *Frontiers in Molecular Neuroscience*, *16*, 1168948. https://doi.org/10.3389/fnmol.2023.1168948

[40] Huang, S., Yang, Z. J., Yu, C., & Sinicrope, F. A. (2011). Inhibition of mTOR kinase by AZD8055 can antagonize

chemotherapy-induced cell death through autophagy induction and down-regulation of p62/sequestosome 1. *The Journal of Biological Chemistry*, *286*(46), 40002-40012. https://doi.org/10.1074/jbc.M111.297432

[41] Xie, Y., Lei, X., Zhao, G., Guo, R., & Cui, N. (2023). mTOR in programmed cell death and its therapeutic implications. *Cytokine & Growth Factor Reviews*, *71-72*, 66-81. https://doi.org/10.1016/j.cytogfr.2023.06.002